IEEE Access
Multidisciplinary | Rapid Review | Open Access Journal

SPECIAL SECTION ON NEW WAVEFORM DESIGN AND AIR-INTERFACE FOR FUTURE HETEROGENEOUS NETWORK TOWARDS 5G

Received June 16, 2019, accepted July 1, 2019, date of publication July 10, 2019, date of current version August 23, 2019.

Digital Object Identifier 10.1109/ACCESS.2019.2927731

Vehicle Lighting Recognition System Based on Erosion Algorithm and Effective Area Separation in 5G Vehicular Communication Networks

ZI-CHUAN YI[1,2], ZHI-BIN CHEN[3], BAO PENG[4], SHI-XIAO LI[3], PENG-FEI BAI[3], LING-LING SHUI[3], CHONG-FU ZHANG[5], (Senior Member, IEEE), AND GUO-FU ZHOU[3]

[1]College of Electron and Information Engineering, University of Electronic Science and Technology of China, Zhongshan Institute, Zhongshan 528402, China
[2]Shenzhen Guohua Optoelectronic Tech Company Ltd., Shenzhen 518110, China
[3]South China Academy of Advanced Optoelectronics, South China Normal University, Guangzhou 510006, China
[4]Shenzhen Institute of Information Technology, Shenzhen 518172, China
[5]School of Information and Communication Engineering, University of Electronic Science and Technology of China, Chengdu 611731, China

Corresponding author: Bao Peng (pengb@sziit.edu.cn)

This work was supported in part by the Key Research Platforms and Research Projects in Universities and Colleges of Guangdong Provincial Department of Education under Grant 2018KQNCX334, in part by the Zhongshan Innovative Research Team Program under Grant 180809162197886, in part by the Zhongshan Institute through the High-Level Talent Scientific Research Startup Fund Project under Grant 416YKQ04, in part by the National Key Research and Development Program of China under Grant 2018YΓB0407100-02 and Grant 2016YΓB0401502, in part by the Guangdong Province Higher Vocational Colleges and Schools Pearl River Scholar Funded Scheme (2016), and in part by the Project of Shenzhen Science and Technology Innovation Committee under Grant JCYJ20170817114522834.

ABSTRACT For the safety of meeting vehicles at night, a design scheme of vehicle lighting recognition system for 5G vehicular communication networks is proposed in this paper. Firstly, a camera is used for image acquisition, and then the acquired RGB image is converted to a hue-saturation-lightness (HSL) image in Dedicated cloud. Secondly, a 3×3 convolution kemel is constructed, and the threshold of this HSL is used to create a mask. In which we traverse the original image data and perform uitwise operations on the original image, as well as mask by using the Urightest point as the center of calculation. Lastly, the effective area of the image is divided according to the farthest point of the lane line extension, which can shield the sky and street lights. In addition, all of interference points are excluded according to the symmetry of the headlights shape, the number of false detection is reduced effectively. So, the highlight areas can be marked to indicate the lights from the front vehicles. The results of the analysis are issued to the driving assistant system. The experimental results show that the system can identify the front vehicle lighting with an accuracy of 96.8%. With the help of the identified lighting position, the matrix lamp is set to realize the dynamic management of the beam, and it can be applied to traffic at night for preventing traffic accidents.

INDEX TERMS Lighting recognition, erosion algorithm, HSL image, bitwise operation, effective area.

I. INTRODUCTION

5G will generate great value in many indusmes such as security monitoring, video services, industrial goods, and smart transportation. Among them, vehicle networking (smart transportation) is a single industry application scenario that can achieve the largest economies of scale. The current Internet ofVehicles is still at Level 3, and more value is reflected in assisted driving and reducing traffic accidents [1]. A vehicle network security application is introduced in this paper based on 5G environment, which is expected to reduce night traffic accidents by more than 30%, and the market size will exceed 1 billion US dollars [2].

In the scene of vehicles meeting at night, the driver's eyes are used to the dark environment, and blindness in an instant may be caused when the eye encounters intense illumination from opposite vehicles suddenly. Hence, traffic accidents are likely to occur in the short time. So, automated auxiliary

The associate editor coordinating the review of this article and approving it for publication was Qilian Liang.

system can be used to remind drivers, and the driving at night is more safety [3]. In the field of automotive intelligent vehicles meeting system, such as ultrasonic radar, millimeter wave radar, laser radar and other detection equipment. Because of a blind zone and interference of oUstacles, the detection range of most detection equipment is limited [4]. Hence, a road detection method which is employed by the multiple reflection intensity of laser radar and machine learning algorithm has been proposed [5]. In this method, due to the diversity of the road surface environment, a long- term data comparison is required. So, its analysis situation is too complicated. With the development of video image processing technology, advanced driving assistant systems (ADAS) have emerged in traffic, such as backing assistant system, rear-end collision waming system, and adaptive driving beam (ADB). Most of these auxiliary systems are based on camera video vehicle detection technology. The most common vehicle detection methods are background subtraction and time difference subtraction [6]. Background subtraction relies on clean background images. The quality of background model directly affects the detection effect of moving objects. The frame difference method relies on the time interval and texture information, and the texture is not clear in the night environment, so as to reduce the effect of target detection.

In vehicle detection, a high-precision vehicle detection mechanism based on robust adaptive vehicle mask training has been proposed [7]. The mask is trained by the combination of color distribution and weighting information, Uut color information is not obvious at night. B. Zhang et al. have used GaUor wavelet transform and Pyramid Histogram of Oriented Gradients (PHOG) to extract features, Uut it requires more computational load [8]. M. Rezaei et al. have proposed a vehicle collision waming system based on real-time monocular vision which can prevent the rear-end situation of vehicles, Uut it is not suitable for the situation of meeting vehicles [9]. Z. Ding et al. have proposed a light pattern descriptor (LPD) to describe the vehicle characteristics for the vehicle type recognition, and it is used as a feature of the vehicle according to the front light position distribution, Uut the detection effect of the occluded vehicle is not satisfactory [10]. R O'Malley et al. have proposed a system based on rear light recognition, which is not suitable for the situation of the vehicle, the light effects of non- vehicle light objects, such as street lights. And the offset of the camera's shooting angle can cause a reduction in recognition effect [11]. W. Zhang et al. have proposed an application of Bouguer optical attenuation model and an improved Laplace of Gaussian (LOG) algorithm for processing the video image [12]. In order to detect the vehicle lighting in Markov random field, this method is not ideal for the reflection suppression effect on the lane and the traffic lights on the road surface. B. Wu et al. have put forward a rule based on vehicle lighting detection algorithm, Uut this algorithm only considered the headlights detection which from the shape angle of vehicle lighting, and it ignored the constraints of multi-frame motion headlight information [13]. Therefore, it cannot avoid the influence of interference light sources such as street lamps. N. Kosaka et al. proposed the Center Surround Extremas method for detecting lighting spots [14]. This method can distinguish the travel direction of the car according to the lane line, the highlights of the car lights and other lights are classified by Support Vector Machine (SVM), and the recognition rate is improved. However, the system also detected many street lights and reflectors incorrectly. In addition, in order to ensure the correct rate, the system requires a large amount of sample data to generate a classifier.

In this paper, a vehicle lighting recognition system based on erosion algorithm and effective area separation is proposed. The camera is used to capture the image data of the road ahead, and red-green-blue (RGB) images are converted to HSL images. Image processing mathematical morphology method is introduced to obtain the edge and erosion center of image. All of irregular reflectors are identified according to the shape symmetry characteristics of the vehicle lighting. By dividing the image into upper and lower parts, we can identify the position of the front vehicle light in the lower half ofroad area in the image. What's more, it is also possible to dynamically adjust the upper and lower boundary lines according to the farthest position of the lane line to adapt to the actual road conditions such as slope and downhill roads. And then, the direction of illumination of matrix headlights can be controlled according to the lighting environment. Liquid crystal display (LCD) and wireless Bluetooth are configured in the proposed system, and the Bluetooth technology is used to interface with the mobile client to achieve picture adjustment. Recognition calibration line which is added to the image display is used to solve the shift problem of shooting angle and optimize the recognition effect. In summary, the system can reduce the number of false recognitions and improve the correct rate effectively.

II. SYSTEM DESIGN PRINCIPLE

In the image processing of mathematics morphology theory method, a structural element with a certain form is used to measure and extract the corresponding shape in the image, then, the effect of image analysis and recognition are achieved. In this paper, mathematical morphology algorithm is used to filter out noise effectively, the edge information is smoother, skeleton is more continuous, and the extracted image is better.

There are two basic operations in morphological operations: Expansion and Erosion. In image processing morphology [15], B is used to expand A for sets A and B in Z, which is called $A \oplus B$, it is defined as (1):

$$A \oplus B = \{z|[(\hat{B})_z \cap A] \subseteq A\} \tag{1}$$

In the expansion formula, each element of image in A is scanned with structure element B, and an OR operation is implemented with its overlaid binary image by using B. A is dilated by B and it is the set of all displacements z, at least one element is overlapping.

In addition, A is eroded with B for sets A and B in Z, which is shown as $A\Theta B$, and it is defined as (2):

$$A\Theta B = \{z|(B)_z \subseteq A\} \tag{2}$$

The erosion formula indicates that erosion of A is executed by using B, the set ofpoints z in A is translated by z.

The Hough transform method is used in the detection and the extraction of straight lines in an image. For each pixel (x, y), all lines $y = kx + b$ which may pass through it are mapped to k-b space (Hough space), and it is mapped to the $\rho - \theta$ space in the polar coordinate system. Then, we use a straight line expression with polar coordinates to represent the line in the image, as shown in (3).

$$p = x_0 \cos(\theta) + y_0 \sin(\theta) \tag{3}$$

In (3), $(xo,\ y_0)$ are the coordinates of the pixel points of an edge on the line in the image. ρ is the distance from the point to the origin, and θ is the angle between the line and the x- axis.

A. IMAGE PREPROCESSING FROM RGB TO HSL

The initial image acquired by the system may be affected in all three parameters RGB values due to different lighting conditions [16]. But in the HSL value of the image, only one parameter of H value is affected. Therefore, in order to improve the stability of the captured image, the image's RGB value variables are converted into HSL variables in image preprocessing. The RGB to HSL variable formula is as follows:

$$\mathrm{h} = \begin{cases} 60^\circ \times \dfrac{\mathrm{g}-\mathrm{b}}{\max - \min} + 360^\circ, & \max = r \ \ g < b \\ 60^\circ \times \dfrac{g-b}{\max - \min} + 0^\circ & \max = r \ \ g \geq b \\ 0^\circ & \max = \min \\ 60^\circ \times \dfrac{\mathrm{r}-\mathrm{g}}{\max - \min} + 240^\circ & \max = b \\ 60^\circ \times \dfrac{\mathrm{b}-\mathrm{r}}{\max - \min} + 120^0 & \max = g \end{cases} \tag{4}$$

$$\mathrm{s} = \begin{cases} \dfrac{\max - \min}{\max + \min} = \dfrac{\max - \min}{2l}, & 0 < l \leq \dfrac{1}{2} \\ 0, & l = 0/\ \max = \min \\ \dfrac{\max - \min}{2 - (\max + \min)} = \dfrac{\max - \min}{2 - 2l}, & l > \dfrac{1}{2} \end{cases} \tag{5}$$

$$l = \frac{1}{2}(\max + \min) \tag{6}$$

In (4), (5), (6), h represents the hue, l represents the Urightness, s represents the saturation. The max and min respectively represent the maximum and minimum values in RGB. After the image conversion, we record the maximum pixel coordinate of the lightness l according to (6), and it is set as the calculation center target point $(X,\ Y)$.

B. PIXEL EDGE ACQUISTION

In order to determine the upper, lower, left, and right boundaries of the high-luminance area of the image, the image is masked to smooth the image. We use the central target point $(X,\ Y)$ as a structural element to erode the image in (2). A 3×3 convolutional kernel is created and the HSL threshold is used to create a mask. The original image and mask are performed uitwise operations with $(X,\ Y)$ as a starting point. The convolution operator is 3×3 for the source image data $f(x,\ y)$, and the calculation of the image data 4 neighborhood average mask is done by the following formula (7):

$$F(x, y) = \frac{Z(x-1, y) + Z(x+1, y) + Z(x, y-1) + Z(x, y+1)}{4} \tag{7}$$

In (7), x and y represent the horizontal and vertical coordinates of the image. By combining (2) and (6), the (8), (9), (10) and (11) are derived from the left, right, low, up direction of the starting point $(X,\ Y)$.

$$Z(x-1, y) | \max\{[\max f(x-1, y) + \min f(x-1, y)]/2\} \subseteq f(x-1, y) \tag{8}$$

$$Z(x+1, y) | \max\{[\max f(x+1, y) + \min f(x+1, y)]/2\} \subseteq f(x+1, y) \tag{9}$$

$$Z(x, y-1) | \max\{[\max f(x, y-1) + \min f(x, y-1)]/2\} \subseteq f(x, y-l) \tag{10}$$

$$Z(x, y+1) | \max\{[\max f(x, y+1) + \min f(x, y+1)]/2\} \subseteq f(x, y+1) \tag{11}$$

Among them, max and min represent the maximum and minimum values of the function respectively. Then, (7) is combined to form (12) and (13), n_1, n_2, n_3, and n_4 respectively represent the distances between the four direction boundaries and the center $(X,\ Y)$.

$$\begin{cases} F(x - n_1, Y) = 0 \\ F(x + n_2, Y) = 0 \\ F(X, y - n_3) = 0 \\ F(X, y + n_4) = 0 \end{cases} \tag{12}$$

$$\begin{cases} x_{\min} = X - n_1 \\ x_{\max} = X + n_2 \\ y_{\min} = Y - n_3 \\ y_{\max} = Y + n_4 \end{cases} \tag{13}$$

The image is flattened in the high Urightness area, as in (7), we traverse the area and use the current pixel as a reference point to determine whether at least one pixel with value 0 in the four directions of the 3 × 3 area, as (12). The reference point is the boundary point, and the coordinates of this boundary point are recorded, until the points of the boundary are found out. Finally, the coordinates of the left, right, upper and lower boundary points obtained by (13), which are $(x_{min},\ Y)$, $(x_{max},\ Y)$, $(X,\ y_{min})$, $(X,\ y_{max})$.

In order to exclude the reflectors, we analyzed the shape characteristics of the vehicle lighting and reflectors, and the

symmetry of the vehicle lighting can be used to distinguish irregularly shaped reflectors. Specifically, the spotlight of the vehicle lighting is round, $n_1 = n_2 = n_3 = n_4$. In reality, the vehicle lighting show more ovals in the system, whether they are round or oval, they all conform to the characteristics ofupper and lower symmetry and bilateral symmetry. And the difference between elliptical edges and the center maximum is controlled in half ofthe maximum radius.

$$|(n_1 + n_2) - (n_3 + n_4)| < \max(n_1, n_2, n_3, n_4)/2 \quad (14)$$

(14) is the distinguishing condition between the vehicle lighting and the other lights which we set, and the max means the maximum value of n_1, n_2, n_3, and n_4.

C. LANE LINE DETECTION

In detecting the lane line, in order to find the farthest point of the lane line, we perform a Hough transform on the image to detect line. In order to get the corresponding (θ, ρ), the pixel coordinates (x, y) of the image are suUstituted into the (3). In the Cartesian coordinate system, the abscissa is θ and the ordinate is ρ. The n pixels' coordinates of the Urightness value $l > 0$ in the image are shown in (15) respectively.

$$\begin{cases} \rho = x_1 \cos(\theta) + y_1 \sin(\theta), & r > 0,\ 0 < \theta < 2\pi \\ \rho = x_2 \cos(\theta) + y_2 \sin(\theta), & r > 0,\ 0 < \theta < 2\pi \\ \cdots \\ \rho = x_n \cos(\theta) + y_n \sin(\theta), & r > 0,\ 0 < \theta < 2\pi \end{cases} \quad (15)$$

In (15), (x_1, y_1), (x_2, y_2), (x_n, y_n) form n sinusoids on the $\theta - \rho$ plane. There are several intersection points among these sinusoids, a certain number of intersection points are selected for corresponding to straight lines in the x-y plane, and the line has the same slope and intercept as the lane line. Then, a number of the point on the line is set to define a lane line. And we can find the farthest point of the lane line on the detected end ofthe lane line.

III. EXPERIMENTAL RESULETS AND DISCUSSION

A. SYSTEM ARCHITECTURE

The vehicle lighting identification system designed in this paper is composed of power module, Bluetooth module, MCU module, camera video input module and matrix lamp [17], which can support external LCD display to realize real-time video display. According to the wireless Bluetooth 4.0 related application and operation mode [18], wireless communication between the system and the mobile device is established. At the same time, a smart phone client application software with simple operation and complete functions is developed to communicate with the system and adjust the LCD display screen. In the design of the matrix lights, the headlights are arranged in 4 rows and 8 columns with a total of 32 LED lights, which can be irradiated in a direction according to the identification area obtained by the erosion algorithm [19]. Then, the hardware is designed based on system framework, and the system physical display is shown in Fig. 1.

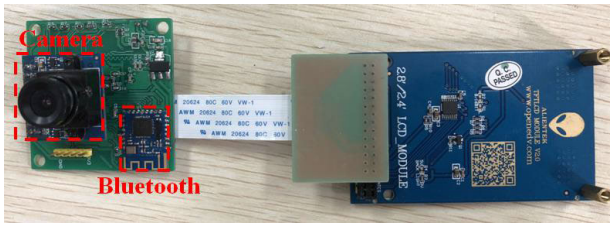

(a) One side of the system.

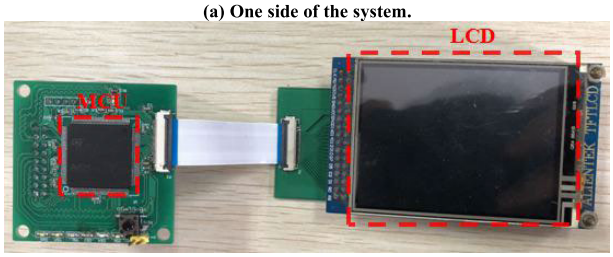

(b) The other side of the system.

FIGURE 1. System physical display.

In addition, the system is designed based on the embedded development platform, the C language program is compiled by the microprocessor, as shown in Fig. 2.

It can be known from the formula in (3) that the lightness is only related to the total amount of the most color components and the least color components of the image. The lower the lightness, the darker the image, and the higher the lightness, the more the area of the image tends to be white.

In a frame of image, there may be many places similar to the Urightness value of the lighting. In order to eliminate the interference point, it is necessary to adjust the range of the maximum Urightness value according to the actual effect. The lower the threshold value, the greater number of satisfied bright spots. The higher the threshold value, the smaller number of satisfied bright spots, and the smaller light area.

B. HIGHLIGHT THRESHOLD SETTING

The Urightness intensity distribution of the vehicle lighting Urightness is analyzed before setting the Urightness value threshold. Fig.3 (a) is the original image. The color temperature component is represented as in (b), the abscissa is x, the ordinate is y, the image pixel maximum value is $x = 1440$, $y = 1080$, and the z axis indicates the color temperature. It can be seen from (c) that there are 9 areas where the color temperature is yellowish, and it can be determined that the vehicle light line may appear in these 9 distribution areas, $x = 40 \sim 60; 120 \sim 380; 700 \sim 730; 750 \sim 820; 960 \sim 980; 1080 \sim 1100; 1200 \sim 1250; 1260 \sim 1330; 1350 \sim 1360$. Since the Urightness ofthe vehicle lighting line should be the strongest in the adjacent position, the range of $x = 120 \sim 380$ can be roughly determined. It can be seen form (d) that the maximum value (yellow) of the vehicle light intensity value of z is around 200, while the larger value (green) is around 150. So, the final initial Urightness threshold is set to 180 in the system.

In the system, since the color of the vehicle lighting is mainly white with high Urightness, the Urightness l is used

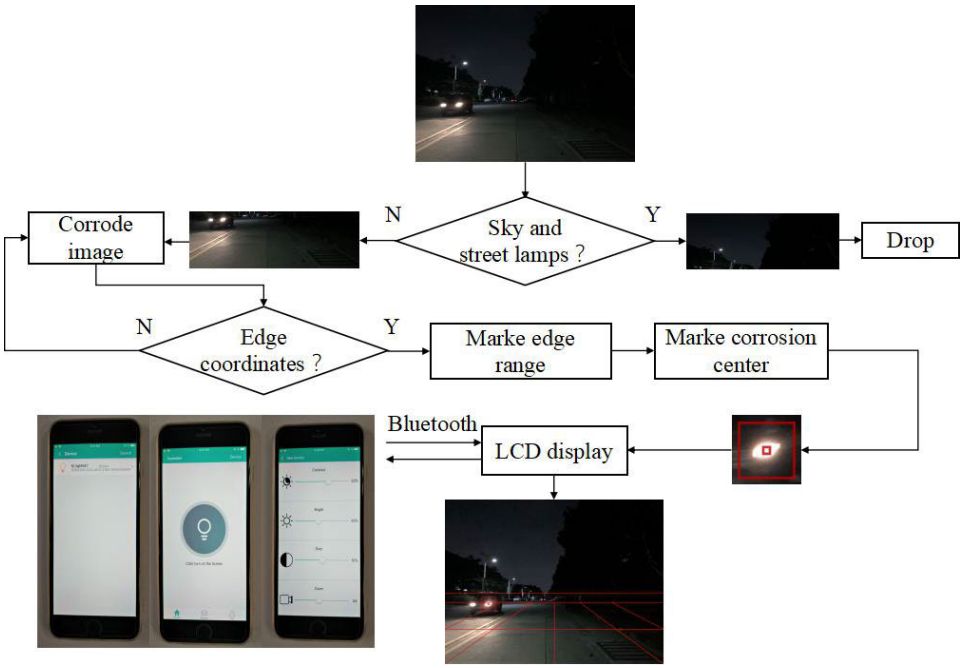

FIGURE 2. System flow chart.

as the main judgment basis in processing image pixel data variables. In image erosion, the image is scanned from top to bottom and left to right for outaining the maximum value of l. The maximum value of l is set as the structural element B in the erosion formula, the entire acquired image is set as A, and it is calculated according to the erosion formula. Finally, the open operation is performed to remove the noise. The specific process is:

The image is scanned to obtain the pixel coordinates with the maximum lightness value l. The pixel coordinates of the left, top, right, and bottom directions are detected from the reference coordinates. If there is at least one l value in the 3×3 region, the reference point is the edge point and this coordinate is recorded in the system. Otherwise, a new reference point is established in the left, up, right, and adjacent directions to detect a new 3×3 area until find the left, right, upper and lower edge values of the vehicle lighting point area, and then, the 4 point coordinates are recorded. The vehicle lighting spot identified in this system is a circle, and the light area can be obtained by using the four-point edge value coordinates.

In the pixel edge acquisition process, the search process usually requires to be iterated a certain number of times on the path from left to right, up to down until 4 edge points are found from the 3×3 range of the reference point. In actual operation, the number of iterations is set as three times. The edge of the light area cannot be searched and the accuracy is low if the number of iterations is too small, the processing speed of the system software may cause the screen to freeze ifthe number of iterations is too large.

C. AREA SEPARATION AND DEBUG

In system deUugging, the corresponding identification is displayed according to the actual road conditions. As shown in Fig. 4 (a), the visual angle is the first perspective. In the figure, the first horizontal line represents the identification of the dividing line. The part above the first horizontal line represents the sky. In order to reduce the calculation of the controller and improve the system response speed, this part is excluded from the overall calculation and it is not identified in the system. The below part of the first horizontal line is the effective area and actual identification range which requires processor operations. The second horizontal line is the calibration line and it is used to align the boundary between the horizontal road surface and the sky in the actual picture when the camera is caliUrated. The third horizontal line, the center vertical line, and the two side lines are all used for road distance reference signs. The physical map is shown in Fig. 4 (b).

The aperture formed by the vehicle lighting on the screen is marked by a large red box when the vehicle on the road and it appears in the identification area. At the same time, the small red box identifies the center of erosion in the image. The experimental phenomena are shown in Fig. 5, it confirms that the system can recognize the vehicle lights successfully.

In order to prove the accuracy of the experimental phenomena, we analyze the light intensity distribution in the lower part of Fig. 5. In Fig.6, it can be seen that the Urightest area is at $x = 200 \sim 270$, followed by $x = 160 \sim 180$, and the area with the Urightest Urightness is selected in the red Uox. The vehicle lights position with the highest Urightness are successfully identified by the system and the final result show

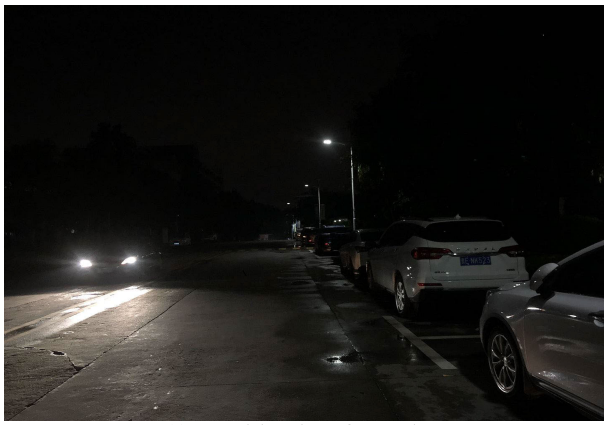

(a) The original light of the vehicle.

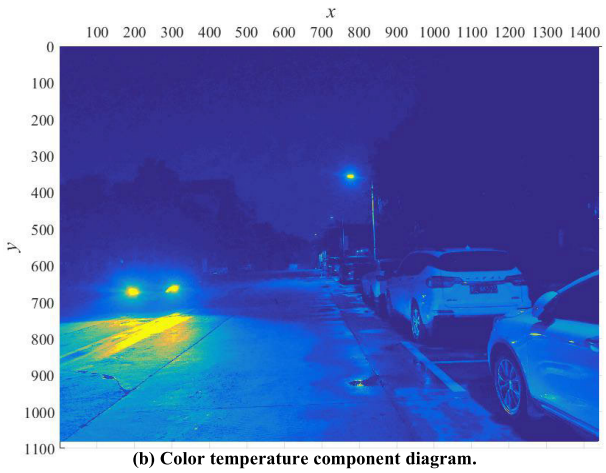

(b) Color temperature component diagram.

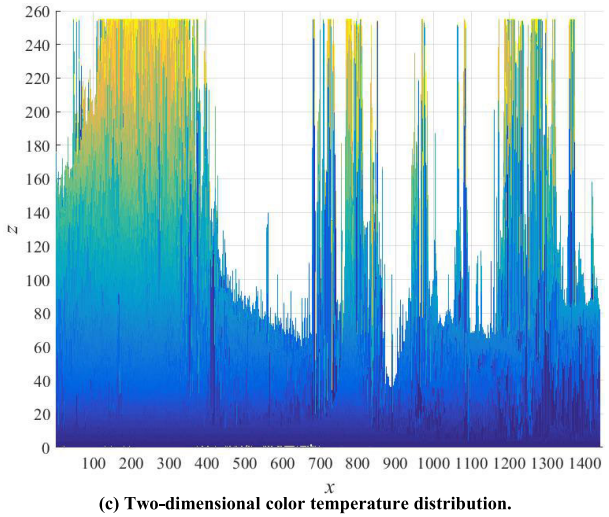

(c) Two-dimensional color temperature distribution.

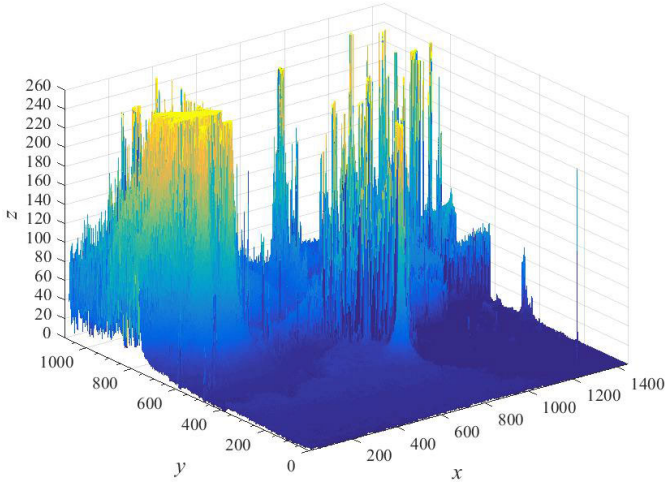

(d) 3D color temperature distribution.

FIGURE 3. Vehicle lighting intensity distribution analysis.

that the size of the identification Uox is appropriate, which can prove that the experimental phenomenon is correct.

D. AREA SEPARATION ENHANCEMENT

The above experiment can successfully detect the headlight of the vehicle, and roughly divide the image area into upper and lower parts, which can avoid the interference of the street lamps, Uut there are also cases where the headlights are missed. In addition, due to the existence of uphill and downhill roads, it cannot exclude street lights and distant non-vehicle light points correctly when the divided area of the image is not accurate.

The method of effective area separation is utilized, and the boundary line is adjusted by the actual situation of the road when the image is required to divide into the sky and the road area. In addition, Linel is set to 1/2 boundary line of the image width by default when the road has no lane line reference. The distance from Linel to Line 2 is set to 1/10 of the width of the image by default (the height of the vehicle in the distance), Line2 should be aligned with the actual boundary line when the system is actually tested and installed.

In Fig. 7, an uphill diagram is shown to explain the content of the effective area separation. In Fig. 7(a), an original image is shown and there is a lane line on the road, the farthest point of the lane extension is used as the horizontal dividing line automatically in the system. The reference point of Line2 is shown in Fig. 7(b), and it is a color converted image. The relative distance between linel and line2 is the approximate height of the vehicle, as shown in Fig. 7(c) and Fig. 7(d). The relative distance between linel and line2 is a constant value and they are overall dynamically adjusted according to the boundary between the actual road and the sky.

In general, in the process of identification, the system excludes invalid areas where the vehicle lightings are impossible appear (above Line1) and the effective area separation is realized for reducing the amount of calculations of the controller. In the proposed method, the interferences such as street lights and traffic control lights are eliminated

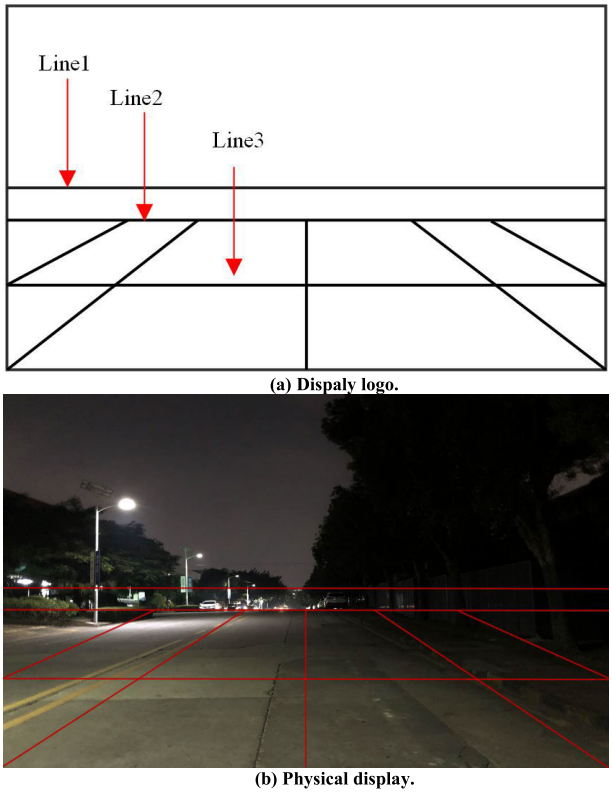

(a) Dispaly logo.

(b) Physical display.

FIGURE 4. Vehicle lighting area marking under road conditions.

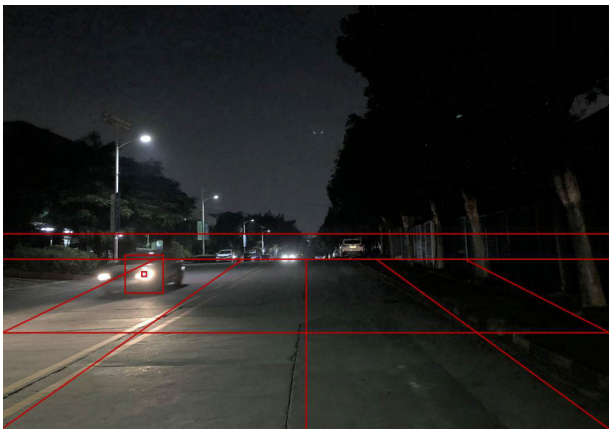

FIGURE 5. Vehicle lighting recognition result display.

effectively. In Fig. 8, the effective area separation in the case of downhill is shown to compare with the Fig. 7.

E. INTERFERENTS DISTINCTION

The bright point symmetry method is introduced to identify the vehicle lighting for distinguishing the reflective objects. According to the shape ofvehicle lighting, it has features of the left and right symmetry and the upper and lower symmetry. The distance between the center of the bright point and four edges (the upper, lower, left, and right) edges are calculated respectively. The distance between the center of the bright spot and the left edge of the bright spot is expressed

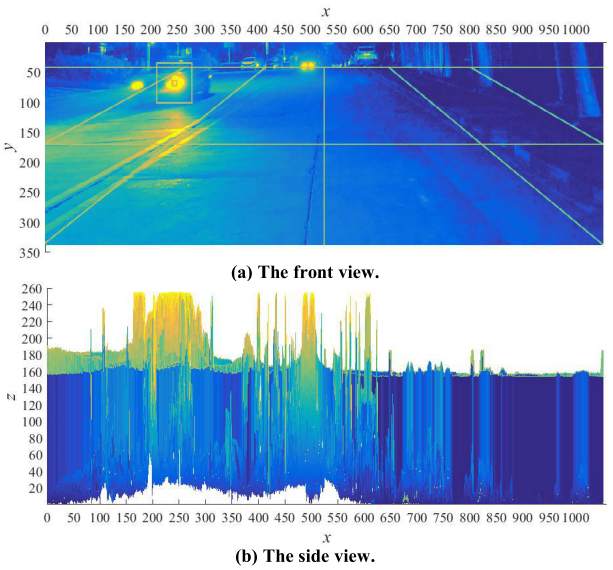

(a) The front view.

(b) The side view.

FIGURE 6. The color temperature of the component.

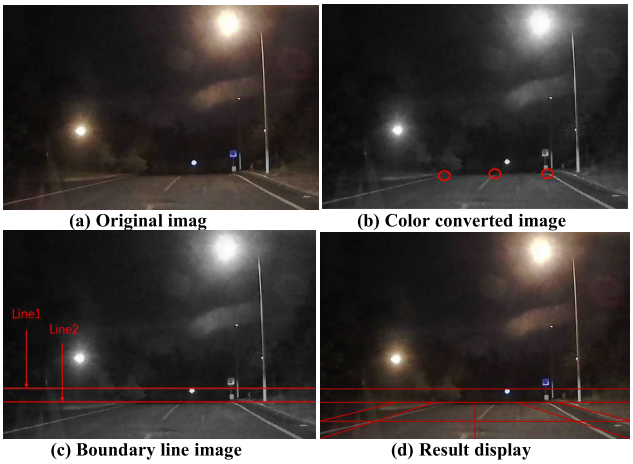

(a) Original imag

(b) Color converted image

(c) Boundary line image

(d) Result display

FIGURE 7. The identification process of effective area separation process in the case of uphill.

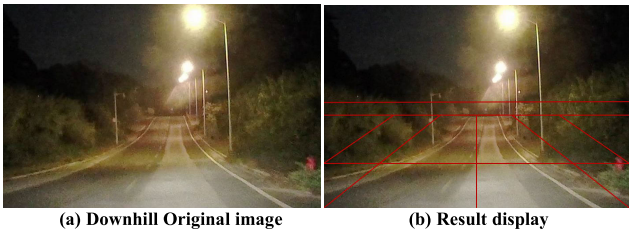

(a) Downhill Original image

(b) Result display

FIGURE 8. The effective area separation in the case of downhill.

as n_1. The distance of the right edge is expressed as n_2, the distance of the upper edge is represented as n_3, and the distance of the lower edge is represented as n_4. And then, the four values are compared. Ideally, $n_1 = n_2, n_3 = n_4$, in actual case, n_1 and n_2, n_3 and n_4 are not equal exactly. But they are not much different, and an error threshold value is set in the system.

We compare the difference between the reflector and vehicle lighting by the following analysis of n_1, n_2 and n_3, n_4.

TABLE 1. Examples of the vehicle lighting recognition.

Examples	Method 1	Method 2	Method 3
1	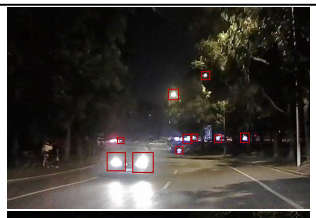	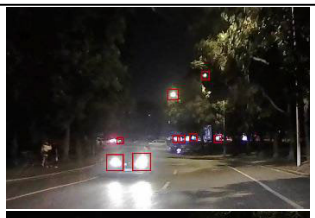	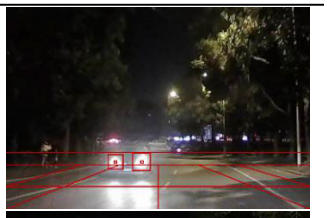
2			
3	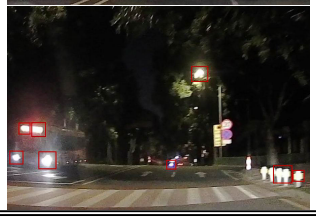		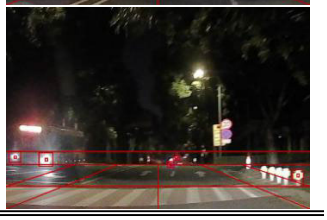

TABLE 2. Comparison of recognition results of vehicle lightings.

Methods	Total number of vehicle lighting	The number of detected vehicle lighting	Error identify number	Accuracy (%)
1	4850	4582	30273	94.5
2	4850	4543	28641	93.7
3	4850	4697	12262	96.8

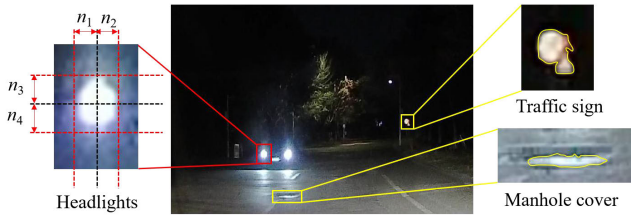

FIGURE 9. Vehicle lighting and reflector shape analysis.

As shown in Fig. 9, the red frame indicates the shape of the vehicle lighting, and the yellow frame indicates the shape of the reflector. We observe that the shape of the near-reflector is irregular, the length and width ofthe reflector are relatively bigger. The differences between the center of the reflector highlight and the four directions edge are not in conformity with the symmemcal rule ofthe lamp light.

F. CONTRAST EXPERIMENTS RESULTS

With the proposed method, a series of comparative experiments are done to illustrate the effectiveness of the proposed system. In TaUle 1, Method 1 is a basic identification system without region division, SVM [12] is used as Method 2, and Method 3 is proposed in this paper.

All the examples show that the proposed method and the traditional method can accurately identify the lights. However, the Method 1 and the Method 2 incorrectly detected small spots in the distance, such as street lights and building lights. The Method 3 can realize effective area separation according to the end ofthe lane line and shield the stray light in the distance for reducing processor operation. In the case of Example 3, both methods incorrectly detected nearby reflective objects such as fire hydrants. In general, the method of this paper can reduce the number of false detections compared with other methods. As shown in TaUle 2, under the same total number ofvehicle lighting, the correct rate of the proposed method is 96.8% and it is higher than that of Method 1 and Method 2. In addition, the number of false detections is significantly reduced. The above results show that the proposed method can improve the accuracy of the system effectively and reduce the false positive rate.

IV. CONCLUSION

A vehicle lighting recognition system based on erosion algorithm is proposed as a basic method in this paper, and a series of system enhancement methods are proposed for improving system accuracy and operation speed. In the system, the road image is collected by a camera, and we perform a series

of processing on the images to detect the front road surface and identify the front vehicle lights. The sky and street lights are shielded selectively by the method of effective area separation, which reduces the burden of processor operations and the light interference of street lights. In addition, the identification line is added on the display to enhance the user experience. So, a safe driving assistance system based on visual image processing is realized, it can provide a friendly man-machine interface, which will be one of the future development directions of intelligent vehicle-borne auxiliary systems.

REFERENCES

[1] IHS Markit Technology Expert, "Vehicular communication networks industry," IHS Markit, London, U.K., Res. Rep., 2019.
[2] *The 5G Economy*. Qualcomm, San Diego, CA, SUA, 2017.
[3] P. Sevekar and S. B. Dhonde, "Night-time vehicle detection for automatic headlight beam control," *Int. J. Comput. Appl.*, vol. 157, no. 7, pp. 8–12, Jan. 2017.
[4] T. Kishigami, T. Morita, H. Mukai, M. Otani, and Y. Nakagawa, "Advanced millimeter-wave radar system to detect pedestrians and vehicles by using coded pulse compression and adaptive array," *IEICE Trans. Commun.*, vol. 96, no. 9, pp. 2313–2322, Sep. 2013.
[5] M. Aki, T. Rojanaarpa, K. Nakano, Y. Suda, N. Takasuka, T. Isogai, and T. Kawai "Road surface recognition using laser radar for automatic platooning," *IEEE Trans. Intell. Transp. Syst.*, vol. 17, no. 10, pp. 2800–2810, Oct. 2016.
[6] S. Sivaraman and M. M. Trivedi, "A general active-learning framework for on-road vehicle recognition and tracking," *IEEE Trans. Intell. Transp. Syst.*, vol. 11, no. 2, pp. 267–276, Jun. 2010.
[7] J.-M. Guo, C.-H. Hsia, K. Wong, J.-Y. Wu, and Y.-T. Wu, "Nighttime vehicle lamp detection and tracking with adaptive mask training," *IEEE Trans. Veh. Technol.*, vol. 65, no. 6, pp. 4023–4032, Jun. 2016.
[8] B. Zhang, "Reliable classification of vehicle types based on cascade classifier ensembles," *IEEE Trans. Intell. Transp. Syst.*, vol. 14, no. 1, pp. 322–332, Mar. 2013.
[9] M. Rezaei, M. Terauchi, and R. Klette, "Robust vehicle detection and distance estimation under challenging lighting conditions," *IEEE Trans. Intell. Transp. Syst.*, vol. 16, no. 5, pp. 2723–2743, Oct. 2015.
[10] Z. Ding and W. Mo, "Vehicle feature recognition based on the frontal lamp pattern descriptor," in *Proc. 2nd IEEE Int. Conf. Comput. Commun. (ICCC)*, Chengdu, China, Oct. 2017, pp. 375–379.
[11] R. O'Malley, E. Jones, and M. Glavin, "Rear-lamp vehicle detection and tracking in low-exposure color video for night conditions," *IEEE Trans. Intell. Transp. Syst.*, vol. 11, no. 2, pp. 453–462, Jun. 2010.
[12] W. Zhang, Q. M. J. Wu, G. Wang, and X. You, "Tracking and pairing vehicle headlight in night scenes," *IEEE Trans. Intell. Transp. Syst.*, vol. 13, no. 1, pp. 140–153, Mar. 2012.
[13] B. Gamma Wu, Y. L. Chen, Y. H. Chen, C. J. Chen, and C. T. Lin, "Real-time image segmentation and rule-based reasoning for vehicle head light detection on a moving vehicle," in *Proc. Signal Image Process.*, Jan. 2005, pp. 389–394.
[14] N. Kosaka and G. Ohashi, "Vision-based nighttime vehicle detection using CenSurE and SVM," *IEEE Trans. Intell. Transp. Syst.*, vol. 16, no. 5, pp. 2599–2608, Oct. 2015.
[15] S. Wang, C. Yan, T. Zhang, and G. Zhao, "Application of mathematical morphology in image processing," *Comput. Appl. Eng. Educ.*, vol. 32, no. 32, pp. 89–92, Jan. 2002.
[16] I-U.-H. Qazi, O. Alata, J.-C. Burie, A. Moussa, and C. Fernandez-Maloigne, "Choice of a pertinent color space for color texture characterization using parametric spectral analysis," *Pattern Recognit.*, vol. 44, no. 1, pp. 16–31, Jan. 2011.
[17] G. Elger, B. Spinger, N. Bienen, and N. Benter, "LED matrix light source for adaptive driving beam applications," in *Proc. IEEE Electron. Compon. Technol. Conf.*, Las Vegas, NV, USA, May 2013, pp. 535–540.
[18] C. Bisdikian, "An overview of the Bluetooth wireless technology," *IEEE Commun. Mag.*, vol. 39, no. 12, pp. 86–94, Dec. 2001.
[19] H. Jing, L. Liu, H. Cheng, and L. Shao, "Morphological ordered grayscale erosion for optical image processing," *Opt. Eng.*, vol. 37, no. 6, pp. 1732–1739, Jun. 1998.

ZI-CHUAN YI received the Ph.D. degree from the Electronic Paper Display Institute, South China Academy of Advanced Optoelectronics, South China Normal University (SCNU), China, in 2015.

He is currently a Researcher with the University of Electronic Science and Technology of China (UESTC), Zhongshan Institute. He has authored or coauthored over 30 papers and holds more than 60 patents. His current research interests include intelligent system design and vehicle electronics.

ZHI-BIN CHEN received the bachelor's degree in electronic information engineering from the Zhongshan Institute, University of Electronic Science and Technology of China (UESTC), in 2017. He is currently pursuing the degree with SCNU.

His research interests include image processing and vehicle electronics.

BAO PENG received the Ph.D. degree in information and communication engineering from the Institute of Electronic Information Engineering, Harbin Institute of Technology, Harbin, China, in 2009.

He is currently an Associate Professor with the Shenzhen Institute of Information Technology. His research interests include the areas of distributed systems and information management.

SHI-XIAO LI received the bachelor's degree in optoelectronic information engineering from the Huazhong University of Technology Wuchang Branch. He is currently pursuing the degree with SCNU.

His research interests include image processing and vehicle electronics.

PENG-FEI BAI received the M.S. and Ph.D. degrees in mechanical and automotive engineering from the South China University of Technology, China, in 2007 and 2010, respectively.

He is currently a Researcher with SCNU. His research interests include the process for display technologies and vehicle electronics.

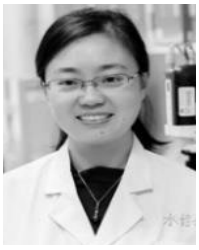

LING-LING SHUI received the B.S. and M.S. degrees in colloid and interface chemistry from Shandong University, in 2000 and 2003, respectively, and the Ph.D. degree in electrical engineering from the University of Twente, The Netherlands, in 2009.

She is currently a Professor with the South China Academy of Advanced Optoelectronics, SCNU, where she works on optofluidics, chemical/biomedical sensors, digital droplet systems, and electrowetting displays.

CHONG-FU ZHANG (SM'15) received the Ph.D. degree from the University of Electronic Science and Technology of China (UESTC), in 2009.

From 2013 to 2014, he was a Visiting Scholar with the OCLAB, University of Southern California. He is currently a Full Professor with UESTC. He has authored or coauthored over 100 papers and holds 40 patents. His research interests include broadband access networks and optical signal processing. He is a member of the OSA.

GUO-FU ZHOU received the M.S. and Ph.D. degrees in functional materials from the Institute of Metal Research, Chinese Academy of Sciences, China, in 1989 and 1991, respectively, and the Ph.D. degree in materials physics from the University of Amsterdam, in 1994.

He was a Visiting Scientist with the University of Cambridge, U.K., before he joined Philips Research, in 1995. He is currently a Professor with the South China Academy of Advanced Optoelectronics, SCNU. He holds more than 100 scientific publications and is an inventor of more than 100 patents in the field of optoelectronic devices and systems. He received the Gold Medal ISMANAM-1994 Grenoble and the 2006 Gilles Holst Award of Royal Dutch Philips.